A Comparative Study of Third-Order Nonlinear Optical Properties of Silver Phenylacetylide and Related Compounds via Ultrafast Optical Kerr Effect Measurements

Boon K. Teo* and Yi Hui Xu

Department of Chemistry, University of Illinois at Chicago, Chicago, Illinois 60607

Bing Yuan Zhong, Yuan Kang He, and Hui Ying Chen

Department of Chemistry, Peking University, Beijing 100871, China

Wei Qian, Yu Jun Deng, and Ying Hua Zou

Department of Physics, Peking University, Beijing 100871, China

Received April 17, 2001

A comparative study of the third-order nonlinear optical properties, via the newly developed heterodyned optical Kerr effect (OHD-OKE) measurements, of silver phenylacetylide and related compounds is reported. $[AgC{\equiv}CC_6H_5]_n$ (**1**) was found to exhibit efficient third-order nonlinear optical susceptibility $\chi^{(3)}$ of 2.4×10^{-14} esu, and second hyperpolarizability γ of 9.07×10^{-32} esu. These results are compared with those of two related silver phenylacetylide compounds, namely, a double salt, (silver phenylacetylide)·(silver *tert*-butylthiolate) $[AgC{\equiv}CC_6H_5{\cdot}AgS(t\text{-}C_4H_9)]_n$ complex (**2**), and a cluster, triphenylphosphine silver phenylacetylide tetramer, $[(C_6H_5)_3PAgC{\equiv}CC_6H_5]_4$ (**3**), as well as that of the related organic polymer polyphenylacetylene (**4**). These four compounds represent different types of phenylacetylide derivatives: **1** is an organometallic polymer, **2** a polymeric double salt, **3** a discrete metal cluster, and **4** an organic polymer. It was found that the third-order optical nonlinear response was enhanced by the incorporation of silver d electrons into the delocalized conjugated organic π system, and its magnitude is highly dependent upon the extent of the π delocalization. Specifically, the relative magnitudes of $\chi^{(3)}$ and γ follow the order silver phenylacetylide polymer (**1**) > (silver phenylacetylide)·(silver *tert*-butylthiolate) double salt (**2**) > polyphenylacetylene polymer (**4**) > tetrameric (triphenylphosphine silver phenylacetylide)$_4$ cluster (**3**). The observed trend may be attributed to the decreasing length of π conjugation. It is interesting to note that the incorporation of Ag(I) into the polymeric framework of polyphenylacetylene enhances the $\chi^{(3)}$ by 25-fold for the same degree of polymerization ($n = 7$). The signs of $\chi^{(3)}$ and γ, which are related to the response mechanisms, were found to be solvent dependent.

Introduction

Recently, special attention has been focused on conjugated organic polymers for their potential in the design and synthesis of advanced materials.[1,2] The π-electron delocalization in conjugated systems contributes to the ultrafast response capability and large third-order nonlinearity. Conjugated polymers with efficient and fast optical response may find applications as fast optical switches and modulators. In the past decade, investigation of functionalized transition metals coordinated with organic ligand systems has intensified due to the expectation that incorporation of d electrons in the conjugated organic system will greatly enhance the hyperpolarizability and the nonlinear susceptibility.[3,4] In this regard, though phenylacetylene and its polymers and copolymers have been widely studied, the corresponding metal phenylacetylides, particularly silver phenylacetylides, have not attracted much attention. The latter is believed to be polymeric with delocalized conjugated σ and π bonding between silver and the triple bonds. Indeed, recent related studies have shown that phenylacetylene and metal phenylacetylides play important roles in the formation of unusual clusters with interesting electronic or optically active properties through bridging or scaffolding.[5−12]

(1) Salaneck, W. R., Stafstrom, S., Bredas, J. L., Eds. *Conjugated Polymer Surfaces and Interfaces, Electronic and Chemical Structure of Interfaces for Light Emitting Devices*; Cambridge University Press: Cambridge, 1996; p 154.
(2) Salaneck, W. R., Landstrom, I., Ranby, B., Eds. *Conjugated Polymers and Related Materials—The Interconnection of Chemical and Electronic Structure*; Proceedings, 81st Nobel Symposium, (June 18, 1991); Oxford University Press: Oxford, 1993; p 502.
(3) Long, N. J. *Angew. Chem., Int. Ed. Engl.* **1995**, *34*, 21−38.
(4) Bruce, D. W., O'Hare, D., Eds. *Inorganic Materials*, 2nd ed.; John Wiley & Sons: Chichester, 1996; pp 122−169.
(5) Yam, V. W. W.; Lee, W. K.; Cheung, K. K. *J. Chem. Soc., Dalton Trans.* **1996**, 2335−2339.
(6) Wang, C. F.; Peng, S. M.; Chan, C. K.; Che, C. M. *Polyhedron* **1996**, *15*, 1853−1858.
(7) Page, H.; Blau, W.; Davey, A. P.; Lou, X.; Cardin, D. J. *Synth. Met.* **1994**, *63* (3), 179−182.
(8) Yam, V. W. W.; Lo, K. K. W.; Fung, W. K. M.; Wang, C. R. *Coord. Chem. Rev.* **1998**, *171*, 17−41.
(9) Chan, W. H.; Zhang, Z. Z.; Mak, T. C. W.; Che, C. M. *J. Organomet. Chem.* **1998**, *556*, 169−172.
(10) (a) Deng, Y.; Xu, Y. H.; Lin, L.; Qian, W.; Xia, Z. J.; Teo, B. K.; Zou, Y. H. *J. Mater. Sci. Lett.* **2000**, *19*, 549−551. (b) Xu, Y. H.; He, X. R.; Hu, C. F.; Teo, B. K.; Chen. H. Y. *Rapid Commun. Mass Spectrom.* **2000**, *14*, 298−303.
(11) Hissler, M.; Connick, W. B.; Geiger, D. K.; Eisenberg, R. *Inorg. Chem.* **2000**, *39* (3), 447−457.

10.1021/ic010408c CCC: $20.00
Published on Web 11/15/2001

We report herein a comparative study of the third-order nonlinear optical properties of silver phenylacetylide and three related compounds via the heterodyned optical Kerr effect (OHD-OKE) measurements. $[AgC{\equiv}CC_6H_5]_n$ (**1**) was found to exhibit efficient third-order nonlinear optical susceptibility $\chi^{(3)}$ of 2.4×10^{-14} esu, and second hyperpolarizability γ of 9.07×10^{-32} esu. These results are compared with those of two related silver phenylacetylide compounds, namely, a double salt, (silver phenylacetylide)·(silver *tert*-butylthiolate) complex, $[AgC{\equiv}CC_6H_5{\cdot}AgS(t\text{-}C_4H_9)]_n$ (**2**), and a tetrameric cluster, triphenylphosphine silver phenylacetylide, $[(C_6H_5)_3PAgC{\equiv}CC_6H_5]_4$ (**3**), as well as that of a closely related organic polymer, polyphenylacetylene (**4**). These four compounds were chosen to represent different types of phenylacetylide derivatives: **1** is an organometallic polymer, **2** a polymeric double salt, **3** a discrete metal cluster, and **4** an organic polymer. It was found that the third-order optical nonlinearity was enhanced by the incorporation of silver d electrons in the delocalized conjugated π system and its magnitude is highly dependent upon the extent of the π delocalization. Specifically, the relative magnitudes of $\chi^{(3)}$ and γ follow the order silver phenylacetylide polymer (**1**) > (silver phenylacetylide)·(silver *tert*-butylthiolate) double salt (**2**) > polyphenylacetylene polymer (**4**) > (silver phenylacetylide)$_4$-(triphenylphosphine)$_4$ cluster (**3**). This latter trend may be attributed to the decreasing length of π conjugation. The signs of $\chi^{(3)}$ and γ, which are related to the response mechanisms, were found to be solvent dependent.

Experimental Section

Reagents. Phenylacetylene (ACROS, 98%) was purified by distillation under nitrogen just prior to use. 2-Methyl-2-propanethiol (*tert*-butyl mercaptan) (ACROS, 99%) was used as purchased.

Instrumentation. Micro FT-IR absorption spectra were recorded with a Nicolet Magna 750 instrument. UV−vis spectra were taken with a Shimadzu 2100 instrument. Elemental analysis was performed with a CARLO ERBA model-1102 instrument. Silver content was determined with inductively coupled plasma atomic emission spectrometry (IRIS AP). ^{1}H nuclear magnetic resonance (^{1}H NMR) spectra were taken with ARX-400. Differential scanning calorimetry (DSC) analysis was done with TA DSC-2010 with a temperature rising rate of 10 °C/min. X-ray photoelectron spectroscopy (XPS) measurements were done with Kratos XSAM 800 (U.K.).

Preparation and Characterization. 1. Preparation of $[AgC{\equiv}CPh]_n$ (1). (a) Two-Step Synthesis. In a 200 mL round-bottomed flask, 0.834 g (4.91 mmol) of silver nitrate was dissolved in 125 mL of acetonitrile to form a colorless solution. NH_3 gas was bubbled through the solution, and white precipitates formed immediately. After about 1 h the NH_3 gas was stopped and 0.65 mL (5.93 mmol) of phenylacetylene was added. The color of the suspension turned to light brown. After stirring for 30 h, the precipitate was collected by filtration, washed with three portions of 50 mL of methyl alcohol, and dried under vacuum. Yield: 0.943 g (91.8%).

Elemental anal. (%) Found (calcd): C, 45.67 (45.98); H, 2.27 (2.41); Ag, 51.0 (51.61).

(b) One-Step Synthesis. Silver nitrate (1.0439 g, 6.15 mmol) was disssolved in 70 mL of acetonitrile in a 100 mL Erlenmeyer flask followed by successive additions of 2.03 mL (18.45 mmol) of phenylacetylene and 2.56 mL (18.45 mmol) of triethylamine with vigorous stirring. The reaction mixture was stirred for 48 h. The white precipitate formed was collected by filtration, washed thoroughly with 3×50 mL of acetonitrile and 3×50 mL of methyl alcohol successively, and dried under vacuum. Yield: 1.118 g (87.07%).

Elemental anal. (%) Found (calcd): C, 45.41 (45.90); H, 2.47 (2.41); Ag, 51.0 (51.61). ^{1}H NMR (323 K, DMSO/$CDCl_3$): 6.821−7.455 (m, $-C_6H_5$).

2. Preparation of $[AgS(t\text{-}Bu)]_n$. To a solution of 22.05 g (0.130 mol) of silver nitrate in 300 mL of acetonitrile, under nitrogen, was added a solution of 49.6 mL (0.44 mol) of *tert*-butylthiol. The resulting white precipitate was collected, washed thoroughly with 3×100 mL methyl alcohol and 250 mL of acetonitrile, and dried under vacuum. Yield: 22.99 g (90%).

Elemental anal. (%) Found (calcd): C, 24.62 (24.38); H, 4.69 (4.60); Ag, 54.70 (54.70). ^{1}H NMR ($CDCl_3$): 1.585 (s, $-C(CH_3)_3$).

3. Preparation of Silver Double Salt $[(AgC{\equiv}Ph)(AgS(t\text{-}Bu))]_n$ (2). Silver *tert*-butyl thiolate (0.11 g, 0.558 mmol) was mixed with a 40 mL solution of 0.12 g (0.558 mmol) of silver phenylacetylide in 1:1 dimethyl sulfoxide (DMSO)/chloroform ($CHCl_3$). The reaction mixture turned silvery-pinkish-beige and was stirred vigorously under nitrogen for 24 h. The precipitate was collected by filtration, washed with ethyl alcohol, and dried under vacuum. Yield: 0.159 g (70.18%).

Elemental anal. (%) Found (calcd): C, 34.45 (35.49); H, 3.26 (3.47); Ag, 53.1 (53.13). ^{1}H NMR (DMSO/$CDCl_3$): 1.534 (s, 9H, $-C(CH_3)_3$), 7.287−7.377 (m, 5H, $-C_6H_5$).

4. Preparation of Tetrameric Cluster $[(Ph_3P)Ag(C{\equiv}CPh)]_4$ (3). Silver phenylacetylide (1.58 g, 7.56 mmol) was suspended in 200 mL of dichloromethane in a 250 mL Erlenmeyer flask with stirring, followed by the addition of 6.016 g (22.94 mmol) of triphenylphosphine. Almost immediately the solid ingredients began to dissolve and the solution became clear and turned pale yellow. The reaction mixture was then stirred in the dark for 4 h. Slow evaporation in the dark afforded colorless crystals, which were collected and recrystallized from dichloromethane. The final product obtained was colorless glistening rectangular columnar crystals with a sharp melting point of 176−178 °C. Yield: 2.86 g (80.3%).

Elemental anal. (%) Found (calcd): C, 66.39 (66.26); H, 4.63 (4.28).

5. Polymerization of Phenylacetylene (4). Phenylacetylene was polymerized by means of molecular sieve NHSY-3 ($SiO_2{\cdot}Al_2O_3{\cdot}Na_2O$, treated with oxalic acid and baked at 300 °C before use). Pulverized NHSY-3 (0.7 g) was placed in a dried polymerization tube. The tube was purged at least four times with pure nitrogen before the pressure in the tube was kept at 0.7 mm Hg. Phenylacetylene (0.8 mL) was then injected into the tube. Polymerization of phenylacetylene occurred immediately and exothermally. The darkened molecular sieve was removed, washed with absolute alcohol, dried, and placed in a plastic container. Dropwise hydrofluoric acid was added into the container to destroy and dissolve the molecular sieve. The resulting light yellow liquid was neutralized with sodium hydroxide to pH 7. The solution mixture was allowed to settle and then extracted with benzene. A viscous liquid thus obtained was redissolved in a minimal amount of benzene, followed by the addition of an excess amount of methanol to precipitate out the product. The reaction mixture was then allowed to stand overnight. The powdered polyphenylacetylene product was obtained by centrifugation and dried under vacuum. Molecular weight determination was performed with vapor pressure osmometry (KNAUER D-1000) at 90 °C, with dimethylformamide (DMF) as solvent. Polyphenylacetylene with an average degree of polymerization 7 was chosen in this study in order to compare with the silver phenylacetylide **1**.

Results and Discussion

Syntheses and Characterization. Four distinct types of phenylacetylene derivatives and/or related compounds have been prepared and studied in this paper. The first is the polymeric silver phenylacetylide (**1**). Generally, **1** can be prepared from the reaction of $[Ag(NH_3)_2]^+$ with phenylacetylene as prescribed in preparation 1(a) in the Experimental Section and in the literature.[13−16] We report here a one-step synthesis of **1** via a homogeneous reaction of silver nitrate with phenylacetylene,

(12) Xu, H. Y.; Tang, B. Z. *J. Macromol. Sci.* **1999**, *36*, 1197−1207.

(13) Brasse, C.; Raithby, P. R.; Russell, C. A.; Wright, D. S. *Organometallics* **1996**, *15*, 639−644.

(14) Osakada, K.; Takizawa, T.; Yamamoto, T. *Organometallics* **1995**, *14*, 3531−3538.

(15) Yam, V. W.-W. *J. Photochem. Photobiol. A* **1997**, *106* (1−3), 75−84.

(16) Yam, V. W. W.; Lee, W. K.; Cheung, K. K. *J. Chem. Soc., Dalton Trans.* **1996**, *11*, 2335−2339.

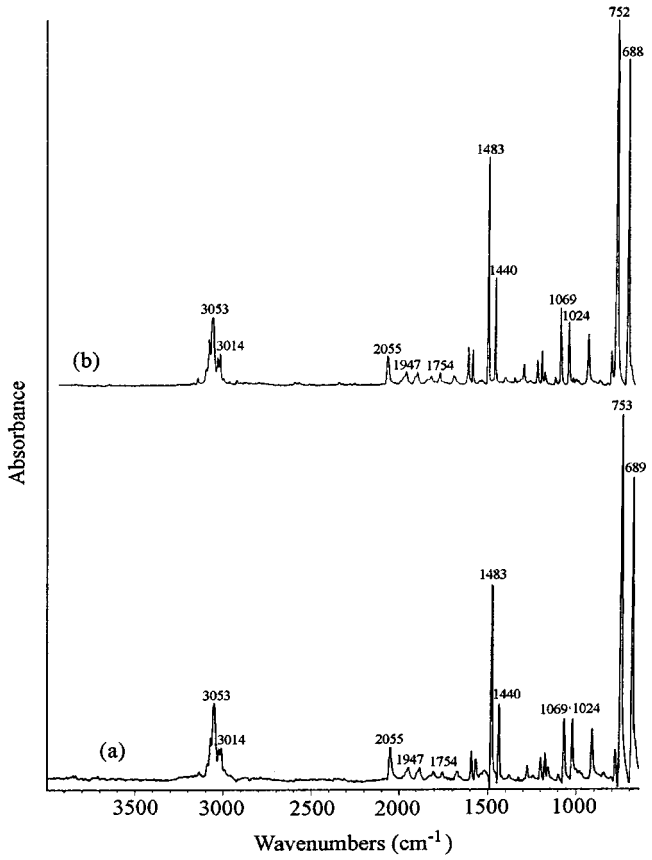

Figure 1. Micro FT-IR spectra of silver phenylacetylide from (a) two-step process and (b) one-step process.

in the presence of triethylamine, resulting in higher purity and better yield. As shown in Figure 1, spectra 1a and 1b of silver phenylacetylide, prepared by the two methods, respectively, are virtually identical. Other than the typical benzene C−H absorption at around 3053, 689, and 753 cm^{-1} and the C=C stretching absorption at 1440 and 1483 cm^{-1}, respectively, there is a set of four weak combination bands at 1754−1947 cm^{-1}, typical of a monosubstituted benzene ring. The acetylene C≡C stretching absorption at 2055 cm^{-1} is consistent with the formation of silver phenylacetylide, $[AgC{\equiv}CPh]_n$. Furthermore, XPS (unpublished results) showed that there is only one kind of silver atom in **1** (Ag $3d_{3/2}$, 374.8 eV; $3d_{5/2}$, 368.8 eV) and, as expected, there are two types of carbons (C 1s, 284.7 and 283.3 eV (sh) in approximately a 3:1 ratio). These spectroscopic results are not inconsistent with the following generally accepted structure of **1** (though other more complicated structures cannot be ruled out).

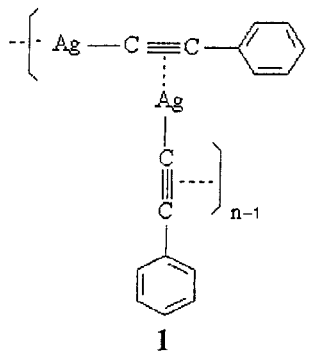

1

The MALDI-TOF mass spectra of silver phenylacetylide had been reported by us (see Figure 1 of ref 10b). There are groups

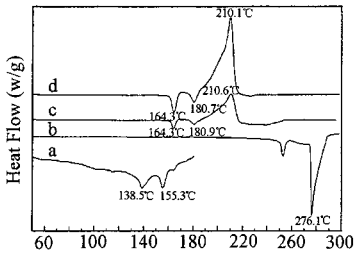

Figure 2. DSC curves of (a) $[AgC{\equiv}CPh]_n$, (b) $[AgS^tBu]_n$, (c) $[(AgC{\equiv}CPh)(AgS^tBu)]_n$, and (d) $[(AgC{\equiv}CPh)(AgS^tBu)]_n$ from a 1:2 $[AgC{\equiv}CPh]_n/[AgS^tBu]_n$ feeding mole ratio.

of intense mass peaks centered at *m*/*z* 315, 523, 731, 939, 1147, etc. Within each group, the peak intensities follow the isotopic distribution expected from the number of silver atoms. (Note that silver has a natural abundance of 51.82% of mass 107 and 48.18% of mass 109.) The mass differences between adjacent groups of peaks are all identical, and equal to the mass number of 218, which is equivalent to a single silver phenylacetylide unit ($AgC{\equiv}CC_6H_5$), or the monomer. This latter observation implies that the monomeric unit remains intact during ionization and acceleration. Moreover, since the *m*/*z* value of each of the molecular ions was exactly 107 Da more than that of the corresponding value of [*n*M] (*n* = integer), the general composition of the molecular ions can be expressed as $[nM + Ag]^+$, where $n = 1, 2, 3, 4, ...$, referred to the degree of oligomerization. As mentioned earlier, each $[nM + Ag]^+$ ion exhibits the expected isotopic distribution of the $(n+1)$Ag atoms, implying that the formation of the observed molecular ions is through the silver cationization.

Due to the higher sensitivity of the linear mode (see Figure 1a of ref 10b), there are detectable molecular ion peaks at up to *m*/*z* 4000, corresponding to a degree of polymerization as high as 20 (though the intensity drops off significantly beyond $n = 7$), whereas in the reflected spectrum (Figure 1b of ref 10b) no detectable mass peaks can be observed beyond *m*/*z* 1600 (which corresponds to $n = 7$).

The second type of compound studied here is the silver double salt $[AgC{\equiv}CPh{\cdot}AgS(t\text{-}Bu)]_n$ complex (**2**). Experimental evidence strongly suggests that the 1:1 adduct $(AgC{\equiv}CPh){\cdot}(AgS(t\text{-}Bu))$, formed by silver phenylacetylide and silver *tert*-butylthiolate, is a"double salt" composite compound. To the best of our knowledge, **2** is the first example of a silver double salt containing both acetylide and thiolate anions. As such, it opens the door to other multiple salts of silver involving these two functional groups. In fact, these two functional groups are highly compatible; and **2** may be considered as a polymeric adduct as indicated by the differential scanning calorimetry (DSC) data depicted in Figure 2 for silver phenylacetylide (curve a), silver *tert*-butylthiolate (curve b), and the $AgC{\equiv}CPh{\cdot}AgS(t\text{-}Bu)$ double salt (curve c). It can be seen that these are distinct compounds, with melting points at 138.5 and 155.3 °C for silver phenylacetylide (**1**) and 252.7 and 276.1 °C for silver *tert*-butylthiolate (**5**). The melting behavior of the $[AgC{\equiv}CPh{\cdot}AgS(t\text{-}Bu)]_n$ double salt is totally different from that of its two constituents **1** and **5**. In curve c, there are two melting points at 164.0 and 180.9 °C and a new exothermal peak with a maximum at 210.6 °C, implying further ordering or polymerization. Thus we can rule out the possibility of a physical mixture of $[AgC{\equiv}CPh]_n$ and $[AgS(t\text{-}Bu)]_n$. Further evidence of this statement was found in our observation that if the feeding mole ratio of $AgC{\equiv}CPh$ to $AgS(t\text{-}Bu)$ was varied, the only product obtained remained the 1:1 adduct, $[AgC{\equiv}CPh{\cdot}AgS(t\text{-}Bu)]_n$, with virtually the same elemental analysis data and DSC thermal transition

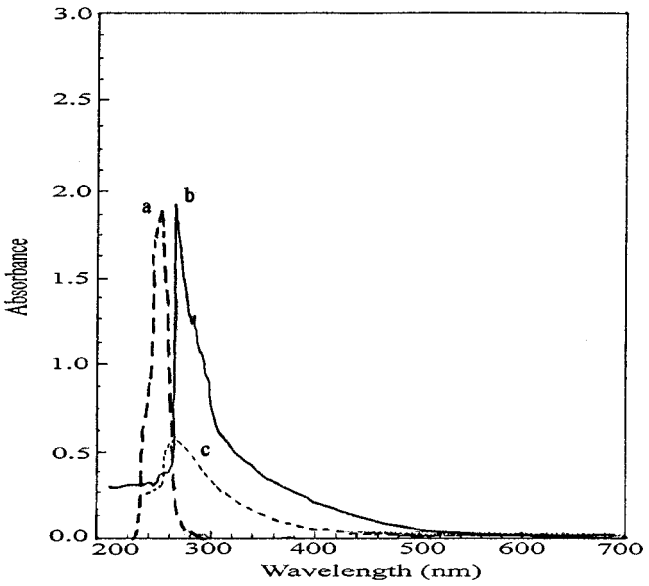

Figure 3. UV−vis absorption spectra of (a) phenylacetylene in 1:1 DMSO/$CHCl_3$; (b) silver phenylacetylide in 1:1 DMSO/$CHCl_3$; and (c) polyphenylacetylene in 1:1:1 DMSO/$CHCl_3$/CH_2Cl_2.

behavior. One such example is shown in curve d of Figure 2 for a 1:2 feeding molar ratio.

The third type of compound studied here is the tetrameric metal cluster $[Ph_3PAgC{\equiv}CPh]_4$ (**3**), which has been synthesized and characterized by one of us.[17] The structure of **3**, as

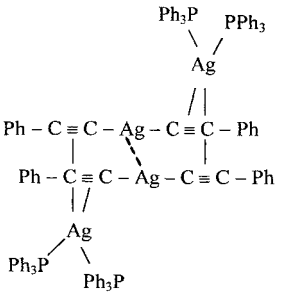

3

determined by single-crystal X-ray crystallography, can be described as two linear anionic $[Ag(C{\equiv}CPh)_2]^-$ units bridged by two $[(Ph_3P)_2Ag]^+$ cationic moieties. The silver atom in each of the two anionic $[Ag(C{\equiv}CPh)_2]^-$ units is σ bonded to the two acetylides in a linear fashion. The silver coordination of the cationic unit may be considered as distorted tetrahedral with two phosphines and two dative π bonds from two C≡C bonds. The four silver atoms form a distorted square with Ag−Ag bonds of 2.9−3.1 Å. It should be mentioned that the overall structure of **3** is similar but not identical to that of $(Ph_3P)_2Ag_2Au_2(C{\equiv}CPh)_4$.[18] In the latter cluster, two linear anionic $[Au(C{\equiv}CPh)_2]^-$ units are bridged by two $[(Ph_3P)Ag]^+$ cationic moieties whose coordination may be considered as a distorted trigonal arrangement of one phosphine ligand and two dative π bonds.

The π conjugated nature of silver phenylacetylide may be illustrated by its UV−vis absorption spectrum in comparison with that of the phenylacetylene, as shown in Figure 3. The absorption maximum of phenylacetylene occurs at 247 nm with no absorption peaks beyond 260 nm (curve a), while the absorption maximum of silver phenylacetylide (**1**) appears at 260 nm and extends somewhat into the visible region with fine structures of two shoulders at 272 and 280 nm (curve b). The observed red shift of the main absorption peak and the occurrence of the fine structures (shoulders) are indicative of an extended conjugated π system of phenylacetylides interacting with the silver d electrons. Specifically, the major absorption band can be assigned to the metal-to-ligand charge transfer (MLCT) involving the excitation of electrons from the filled metal d orbitals (Ag(I) d^{10} configuration) to the virtual π^* orbitals of the C≡C bonds. This MLCT will be referred to as (Ag) $d^{10} \rightarrow \pi^*$ (C≡C) or, simply, $d^{10} \rightarrow \pi^*$ transitions in later discussions.

It is interesting to note that, in a 1:1:1 DMSO/$CHCl_3$/CH_2Cl_2 mixed solvent system, the absorption curve of silver phenyacetylide (**1**) is also a broadened peak with a maximum absorption at 270.6 nm and extends into 350 nm, while that of the tetrameric triphenylphosphine silver phenylacetylide cluster (**4**) is a narrow peak with an absorption maximum at 257.0 nm with no absorption beyond 300 nm. For the (silver phenylacetylide)·(silver *tert*-butylthiolate) double salt (**2**), the absorption peak is also quite broad with a maximum at 270.7 nm and extends to 350 nm. This behavior is similar to that of silver phenylacetylide, indicating that there exists charge transfer in these two compounds. Finally, though the absorption of polyphenylacetylene (**4**) is much weaker than that of the phenylacetylide-containing compounds, it has a broad absorption peak with a maximum at 260.8 nm and extends into 400 nm (curve c in Figure 3), also indicating an extended π conjugated system, but involving C=C bonds instead of C≡C bonds.

Ultrafast Optical Kerr Measurements. In this study, third-order optical nonlinear susceptibilities of silver phenylacetylide (**1**) and three related compounds (**2**−**4**) were investigated via femtosecond optically heterodyned optical Kerr effect (OHD-OKE)[19−21] measurements. In general, third-order optical nonlinear susceptibility $\chi^{(3)}$ is a complex quantity. However, for the majority of photonics applications, such as all-optical switching, signal processing, and data storage, the real components of $\chi^{(3)}$ are more relevant. Unfortunately, in conventional optical Kerr effect (OKE) experiments, the detected signal is proportional to the quadratics of the third-order optical nonlinear susceptibility $\chi^{(3)}$. Hence, the real components of $\chi^{(3)}$ cannot be determined directly from the experiment. Recently, by introducing a local oscillator field with or without 90° optical phase bias with respect to that of optical Kerr signal, a new experimental technique called optically heterodyned optical Kerr effect (OHD-OKE) has been developed. This new technique allows the determination of the magnitudes and signs of both the real and the imaginary components of $\chi^{(3)}$ with greatly improved signal-to-noise ratios.

The experimental arrangement for OHD-OKE, shown in Figure 4, is basically the same as that of OKE, which has been described elsewhere.[22] The laser source is an ultrafast dye laser synchronously pumped by a CW mode-locked Nd:YAG laser operating at 76 MHz. The average power of the output is about 160 mW with wavelength of 647.0 nm. The full width at half-maximum of pulses is about 165 fs, which is deduced from a

(17) Teo, B. K.; Dang, H.; Zhang, H. To be published.
(18) Abu-Salah, O.; Knobler, C. B. *J. Organomet. Chem.* **1986**, *302*, C10−12.
(19) Orczyk, M. E.; Samoc, M.; Swiatkiewicz, J.; Prasad, P. N. *J. Chem. Phys.* **1993**, *98*, 2524−2533.
(20) Orczyk, M. E.; Swiatkiewicz, J.; Huang, G.; Prasad, P. N. *J. Phys. Chem.* **1994**, *98*, 7307−7312.
(21) Lin, L.; Qian, W.; Wang. C. F.; Zou, Y. H.; Wang, Q.; Chen, H. Y. *SPIE* **1999**, *3796*, 131−142.
(22) Yuan, P.; Xia, Z. J.; Zou, Y. H.; Qiu, L.; Shen, J. F.; Xu, J. H. *Chem. Phys. Lett.* **1994**, *224*, 101−105.

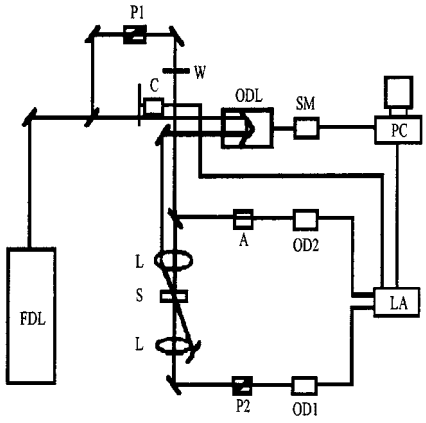

Figure 4. Femtosecond optical Kerr effect experimental arrangement. FDL: femtosecond laser. W: λ/4-plate. S: sample. P1: polarizer. P2: polarization analyzer. C: chopper. ODL: optical delay line. SM: step motor. L: lens. OD1, OD2: photoelectronic diodes. LA: lock-in amplifier.

pump−probe autocorrelation curve measured by second-harmonic generation in KDP at the sample position. The probe and pump pulses are split from the dye laser output (I_{probe}:I_{pump} = 1:7). The probe beam is passed through a polarizer, P1, whose polarization direction is directed at 45° with respect to that of the pump beam. The pump beam is chopped at 2770 Hz, and the probe beam goes through a motorized optical delay line controlled by a computer. The two beams are focused on the same spot of the sample with a spot size of about 10 μm by a lens with a 5 cm focal length. A polarization analyzer, P2, is placed behind the sample at the cross polarization with respect to the input polarizer P1 in order to filter out the residual probe beam. The signal is finally detected by a photodiode connected with a lock-in amplifier and stored in the computer equipped with an analog-to-digital card. As mentioned above, in order to measure the real components of $\chi^{(3)}$ we need to provide a local oscillator field with a 90° optical phase bias with respect to that of optical Kerr signal. To convert from the OKE to the OHD-OKE experimental setup, we insert a quarter-wave plate W between the input polarizer P1 and the focusing lens L. The optic axis of the quarter-wave plate is also directed at 45° with respect to the polarization direction of the pump beam. Through slight rotation of the input polarizer P1, a local oscillator field with a 90° optical phase bias with respect to that of optical Kerr signal can be generated. We define the angle Φ between the polarization direction of polarizer P1 and the optic axis of quarter-wave plate W as the "heterodyning angle."

In our experiment, we measure the time evolution of the intensity of the heterodyned Kerr signal by varying the delay time between the pump and the probe pulses at several heterodyning angles. According to the basic principle of OHD-OKE, the dependence of the intensity, $I(\Phi)$, of the heterodyned Kerr signal, at zero delay time, on heterodyning angle, Φ, can be fitted with the functional form

$$I(\Phi) = Z_1 + Z_2\Phi \tag{1}$$

Thus, by measuring the intensities of the heterodyned Kerr signals (at zero delay time) at two different angles Φ_1 and Φ_2, we can determine the value of Z_2, as follows:

$$Z_2 = (I(\Phi_1) - I(\Phi_2))/(\Phi_1 - \Phi_2) \tag{2}$$

Finally, the coefficient Z_2 is proportional to the real component of $\chi^{(3)}$, as follows:

$$Z_2 = (-4\pi^2\omega^2 d/\kappa_1 c^3)R_2 n^{-1/2}(\chi^{(3)}_{eff})_{real} I_2 I_1 \tag{3}$$

Here I_1 and I_2 are the pump and probe beam intensities, respectively; d is the thickness of the sample cell; κ_1 is the value of the probe beam wave vector; R_2 represents a correction factor for the attenuation of beams in the sample due to linear absorption; n is the index of refraction of the sample; and $(\chi^3_{eff})_{real}$ is the real component of the effective third-order nonlinear optical susceptibility of the sample. From eq 3, we know that if we select a standard sample as reference we can derive the following formula:

$$(\chi^{(3)}_{eff,s})_{real} = \left(\frac{n_s}{n_{ref}}\right)^{1/2}\frac{d_{ref}Z_s}{d_s Z_{ref}}(\chi^{(3)}_{eff,ref})_{real} \tag{4}$$

Here, the subscripts s, ref, and real denote the sample, the reference, and the real component of third-order nonlinear susceptibility, respectively. In our experiment, $d_{ref} = d_s = 80$ μm, n_{ref} and $(\chi^{(3)}_{eff,ref})_{real}$ are known, and Z_s and Z_{ref} can be calculated from the experiment signals. Due to the very low concentration (about 10^{-4} M) of the sample in the solution, the index of refraction of the sample solution, n_s, can be assumed to be the same as that of the solvent. From eq 4, the value of $(\chi^{(3)}_{eff,s})_{real}$ can be determined.

For a dilute solution, the real part of the second hyperpolarizability γ of the solute can be deduced from

$$\gamma_{real} = \frac{\chi^{(3)}_{real}}{N_c L} \tag{5}$$

where N_c denotes the number density of the sample molecules and L is the local field correction factor, which may be approximated by the Lorentz expression,

$$L = (n^2 + 2)/3 \tag{6}$$

Figure 5 shows the OHD-OKE signals of silver phenylacetylide **1** and the related compounds **2** and **4**. Cluster **3** is not shown because it exhibits a negligible third-order optical nonlinear response. Numerical results of the OHD-OKE measurements, along with the absorption maxima in the electronic spectra (Figure 3), are listed in Table 1. From Table 1, it can be seen that the absolute magnitude of the $\chi^{(3)}$ or γ values of these compounds follows the order of silver phenylacetylide (**1**) > (silver phenylacetylide)·(silver *tert*-butylthiolate) (**2**) > polyphenylacetylene (**4**) > (triphenylphosphine silver phenylacetylide)$_4$ cluster (**3**). This decreasing order can be attributed to the extent of conjugation, or, equivalently, to a reduction in effective length of electron delocalization. The largest $\chi^{(3)}$ or γ values were observed in **1**, presumably due to its high degree of conjugation as a result of oligomerization ($n > 7$). The second largest $\chi^{(3)}$ or γ values were observed in **2**, though reduced by a factor of 2. This reduction in the absolute values of $\chi^{(3)}$ or γ values in going from **1** to **2** may be taken as an indication that the extent of conjugation is greatly reduced or impeded as a result of the double salt formation. It is also interesting to note from Table 1 that **1** and **2** have the same signs for $\chi^{(3)}$ or γ and follow the same solvent-induced sign changes (vide infra). Furthermore, the conjugated system composed of repeat units of [AgC≡CPh], as in **1** and **2**, seems to be more effective than that comprising alternating carbon−carbon double bonds as in polyphenylacetylene **4**. Finally, since only two C≡C units are involved in the conjugation, mediated by a silver atom, in a linear fashion (i.e.,

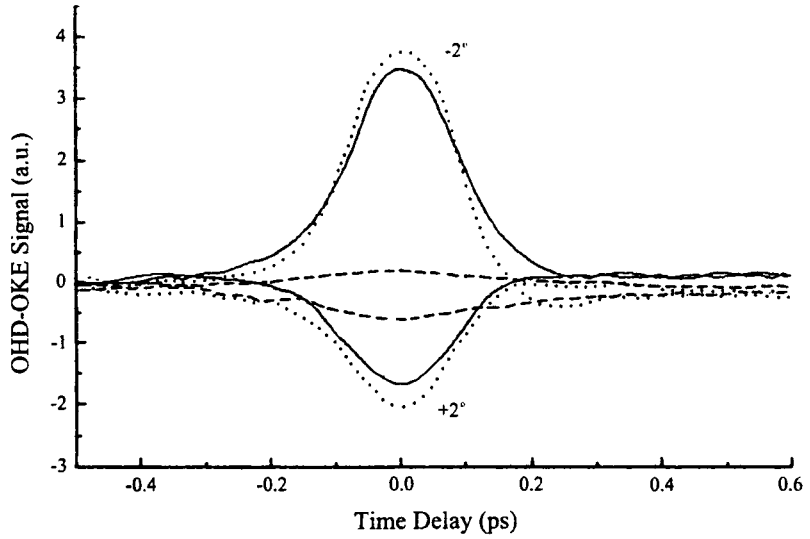

Figure 5. OHD-OKE signals of silver phenylacetylide (—), (silver phenylacetylide)·(silver *tert*-butylthiolate) complex (···) and polyphenylacetylene (- - -).

Table 1. The Absorption Maximum in UV−Vis Spectra, Third-Order NLO Susceptibility ($\chi^{(3)}$), and Second Hyperpolarizability (γ) of Silver Phenylacetylide and Its Derivatives

compound	λ_{max} (nm)	solvent[a]	$\chi^{(3)} \times 10^{-14}$ esu	$\gamma \times 10^{-32}$ esu
$[AgC{\equiv}CPh]_n$	260.0	*a*	2.40	9.07[c]
	270.6	*b*	−1.11	−10.59[c]
$[AgC{\equiv}CPh{\cdot}AgS(t\text{-}Bu)]_n$	264.0	*a*	1.10	7.44[c]
	270.7	*b*	−0.68	−6.49[c]
$[Ph_3PAgC{\equiv}CPh]_4$	257.0	*b*		
$[-CH{=}C(Ph)]_7$	260.8	*b*	0.094	0.52

[a] Solvent systems: (a) 1:1 DMSO/$CHCl_3$; (b) 1:1:1 DMSO/$CHCl_3$/CH_2Cl_2; (c) assume n = 7.

[PhC≡CAgC≡CPh]) in the tetrameric cluster **3**, it has the smallest $\chi^{(3)}$ or γ values.

The signs of $\chi^{(3)}$ and γ deserve some comments. As can be seen from Table 1, both $\chi^{(3)}$ and γ exhibit positive values when 1:1 DMSO/$CHCl_3$ (solvent system a) was used as the solvent system but change to negative values when 1:1:1 DMSO/$CHCl_3$/CH_2Cl_2 (solvent system b) was used. This sign change (from positive to negative) as a result of the slight increase in polarity of the solvent system (from a to b) is rather interesting. Since the structure−property relationships of the third-order NLO materials are not so well understood as those for the second-order NLO materials, models for elucidating the response mechanism for linear conjugated molecules have been suggested. According to Marder and Dirk,[23,24] at least three terms are needed to describe the third-order nonlinear hyperpolarization, i.e., a negative term related to the transition between the ground state and the first excited state, a two-photon term, and a dipolar term. The absolute value of γ depends on the competition of contributions from these three terms. When the two-photon contribution dominates, the susceptibility is expected to be positive, while when the negative term dominates, the susceptibility should be negative. Thus, positive values of susceptibilities are commonly observed for centrosymmetric conjugated structures, while negative susceptibilities are observed, though less frequently, in systems with an odd number of atoms in the conjugated unit. In our experiments, instead, the signs of $\chi^{(3)}$ and γ change from positive to negative with a minor change in the polarity in the solvent system. (The electronic spectra, discussed above, are consistent with the notion that the solvent system of 1:1:1 DMSO/$CHCl_3$/CH_2Cl_2 is more polar than that of 1:1 DMSO/$CHCl_3$.) Hence we conclude that the overall sign of the susceptibility is highly solvent dependent.

Finally, it can be seen from Figure 5 that the signal profiles of all compounds studied here are approximately symmetric with respect to the delay time, implying a primarily pulse width limited response, and, since the time constants of all samples are less than the pulse duration, it is concluded that the relaxation time of all samples is shorter than the laser pulse width (165 fs), which means that the ultrafast optical response originates from the electron movement and/or is caused by distortion of the electron densities. The origin and/or mechanism of such dependence is currently under investigation.

Design Strategies for Third-Order Nonlinear Optical Materials Based on Silver Acetylides. The title compounds **1**−**4** were deliberately chosen for their commonalities and their differences. They were selected to represent four distinctive types of chemical species: **1** being an organometallic polymer, **2** a polymeric double salt, **3** a discrete metal cluster, and **4** an organic polymer. Despite their structural and chemical diversities, compounds **1**−**3** share the common characteristics of having an extended π conjugation system composed of the highly polarizable metal ion (Ag(I), d^{10} configuration) and unsaturated organic ligand (phenylacetylide). These characteristics are known to give rise to highly efficient nonlinear optical properties. The diverse structural types of compounds **1**−**4** allow us to assess the relative importance of stereochemical and electronic factors that may impact the third-order nonlinear optical properties, namely, $\chi^{(3)}$ and γ. On the basis of our results, the following design criteria for metal acetylide derivatives as nonlinear optical materials can be formulated.

First, since high polarizability is key to nonlinear optical responses, it is advantageous to choose metals with a completely filled d shell. Though our focus in this paper was on Ag(I), other d^{10} transition metals such as Cu(I) and Au(I) as well as Zn(II), Cd(II), and Hg(II) are also excellent candidates. It is interesting to note that the incorporation of Ag(I) into the

(23) Dirk, C. W.; Cheng, L.-T.; Kuzyk, M. G. *Int. J. Quantum Chem.* **1992**, *43*, 27−36.
(24) Marder, S. R.; Torruellas, W. E.; Blanchard-Desce, M.; Ricci, V.; Stegeman, G. I.; Gilmour, S.; Bredas, J. L.; Li, J.; Bublitz, G. U.; Boxer, S. G. *Science* **1997**, *276*, 1233−1236.

polymeric framework of polyphenylacetylene enhances the $\chi^{(3)}$ by 25-fold for the same degree of polymerization ($n = 7$). Similarly, although we selected phenylacetylene as the organic ligand, other unsaturated organic molecules with highly polarizable π electrons can also be used. The combination of d^{10} transition metals and triple bonds gives rise to colorless materials covering a wide spectral range (transparent in the near-ultraviolet regime down to 270 nm, the entire visible spectrum, and the near-infrared region up to 3.3 μm). This wide window of optical transparency is highly desirable for laser applications.

Second, the low-lying π^* orbitals of the C≡C triple bond give rise to strong metal−ligand charge transfer (MLCT) transitions that contribute to the nonlinear optical behavior of this class of compounds. Hence, it is advantageous to minimize the excitation energies (ΔE) of these MLCT bands and to maximize their extinction coefficients. Fortunately, for these organometallic compounds, the MLCT occur at about 260 nm (near-UV region) and the extinction coefficients are very high (on the order of 10^5).

Third, it is desirable to maximize the extent of π delocalization. In the case of compound **1**, the degree of oligomerization n is estimated to be 7. Previous work on the nonlinear optical properties of organic polymers suggests that $\chi^{(3)}$ or γ is highly dependent upon the degree of oligomerization n. For example, the ultrafast time-resolved optical Kerr effect had been used to determine the nonresonant third-order optical nonlinearity of polybenzonitrile at a wavelenth of 467 nm.[25] A power-law dependence of $\chi^{(3)}$ or γ on the average degree of polymerization n in the form of $\gamma = an^b$, where $b = 2.4$, was obtained. The results indicate that $\chi^{(3)}$ or γ increases rapidly (faster than quadratic, or, as a power of 2.4) by 5-fold as the average degree of polymerization n increases by 2-fold (from $n = 4.5$ to $n = 9.1$), before tapering off at n greater than 10. Therefore, we anticipate significant improvements of $\chi^{(3)}$ and γ for this class of materials involving silver phenylacetylides as the degree of polymerization n increases. As n increases, the effective π conjugation length increases and the excitation energies (ΔE) of the MLCT bands decrease, resulting in significant enhancement of the third-order nonlinear optical responses.

Fourth, the ligand arrangement of the Ag coordination in compounds **1** and **2** is presumably of an asymmetric nature, with one σ and a number (m) of π interactions, which may be designated as ($\sigma + m\pi$). This arrangement is preferred over the symmetrical arrangement observed in compound **3**, since the asymmetric arrangement of the ligands around the metal atom produces asymmetric electronic distribution which is a desirable attribute for nonlinear optical properties. In **3**, each of the two central silver atoms is σ bonded to two acetylides in a linear fashion (designated as 2σ) whereas each of the two peripheral silver atoms interacts with two acetylenes via π bonding (designated as 2π). The 2σ-type symmetrical ligand arrangement gives rise to very weak third-order nonlinear optical responses.

Fifth, while metal−metal bonding may contribute to electron delocalization in the cluster or polymer, it plays a minor role here since Ag(I), with a filled d orbital manifold (d^{10}), forms weak Ag···Ag interactions, if any, at approximately 3.0 Å. Metal−metal bonding may become important if a large ensemble of metal atoms form a cluster with strong metal−metal bonds.

Finally, this particular class of silver phenylacetylide compounds, especially **1** and **2**, is amenable to molecular and crystal engineering. For compound **1**, substituents could be put on the phenyl group or the acetylene itself. This may affect the mode of bonding, the degree of oligomerization, the excitation energies of the MLCT bands, etc., making this class of materials highly tailorable. Compound **2** is a double salt involving silver acetylide and silver mercaptide, (AgCCR)·(AgSR′) where R = Ph and R′ = *t*-Bu. Highly promising classes of nonlinear optical materials can be generated by combining silver acetylides with other silver salts to form double, triple, and quadruple salts with a wide variety of structures. It is known that silver(I) forms multiple salts of the following general formulas: double salts, *m*AgX·*n*AgY; triple salts, *m*AgX·*n*AgY·*p*AgZ; and quadruple salts, *m*AgX·*n*AgY·*p*Ag·*q*AgW. Related to **2** are the double salt Ag_2C_2·8AgF,[26] the triple salt Ag_2C_2·AgF·4$AgSO_3CF_3$·RCN (R = Me, Et),[27] and the quadruple salt $2Ag_2C_2$·3AgCN·15$AgCO_2$-CF_3·2$AgBF_4$·9H_2O.[28] For these highly interesting multiple silver salts involving the acetylide dianion $(CC)^{2-}$, "argentophilicity"[29] promotes the formation of polyhedral cages of Ag(I) ions that enclose the acetylides, which exhibit a wide range of coordination modes via σ, π, or mixed ($\sigma + \pi$) bonding with the metal ions. For multiple silver salts involving the monosubstituted acetylide monoanion $(CCR)^-$, as in **2**, partial cage formation due to argentophilicity of Ag(I) ions will affect the composition as well as the structure of the resulting polymer. More important for our purpose, however, is the fact that each component of the multiple silver salts can be separately engineered by attaching various different substituents to the anionic ligands. For example, a triple silver salt of the general formula (AgCCR)·(AgSR′)·($AgSO_3$R″) will have three tailorable substituents R, R′, and R″. Similarly, a quadruple silver salt of the general formula (AgCCR)·(AgSR′)·($AgSO_3$R″)·($AgCO_2$R‴) will have four tailorable substituents R, R′, R″, and R‴.

It should be emphasized that the above-mentioned criteria/factors are not totally independent or mutually exclusive. For example, an asymmetric ligand bonding mode may, under favorable conditions, produce a higher degree of oligomerization and smaller MLCT excitation energies, thereby enhancing the nonlinear optical properties.

In summary, for derivatives of compound **1**, in order to achieve high nonlinear optical activity, it is advantageous to place substituents on the phenyl or the acetylene group that will lead to a polymer with a lower MLCT excitation energy, an asymmetric silver coordination, and a large degree of oligomerization. Similar arguments apply to double, triple, and quadruple silver salts, but with the added dimensionalities of molecular design and crystal engineering on each component of the multiple silver salts. These materials have the advantage of versatility and flexibility in design and fabrication. Furthermore, though not emphasized in this paper, these materials can be cast into oriented thin films with highly anisotropic physical properties. Finally, we believe that the stereoelectronic principles and the design strategies developed here are generally applicable to other organometallic polymers as well and, hopefully, will lead to the discoveries of new materials with highly efficient nonlinear optical properties.

Conclusion

It can be seen from the present work that silver phenylacetylide and its derivatives are promising third-order nonlinear optical

(25) Wang, C.; Zhao, X.; Chen, H.; Ai, X.; Xia, Z.; Zou, Y. *Appl. Phys.* **1997**, *B64*, 4548.

(26) Guo, G. C.; Zhou, G. D.; Wang, Q. G.; Mak, T. C. W. *Angew. Chem., Int. Ed.* **1998**, *37*, 630.

(27) Wang, Q. M.; Mak, T. C. W. *J. Am. Chem. Soc.* **2000**, *122*, 7608.

(28) Wang, Q. M.; Mak, T. C. W. *J. Am. Chem. Soc.* **2001**, *123*, 1501.

(29) (a) Pyykko, P. *Chem. Rev.* **1997**, *97*, 597. (b) Omary, M. A.; Webb, T. R.; Assefa, Z.; Shankle, G. E.; Patterson, H. H. *Inorg. Chem.* **1998**, *37*, 1380.

materials. The relative magnitudes of $\chi^{(3)}$ and γ follow the order silver phenylacetylide polymer (**1**) > (silver phenylacetylide)·(silver *tert*-butylthiolate) double salt (**2**) > polyphenylacetylene polymer (**4**) > tetrameric (triphenylphosphine silver phenylacetylide)$_4$ cluster (**3**). It was found that the third-order optical nonlinear response is very fast (in the femtosecond regime) and that the $\chi^{(3)}$ and γ values are correlated with (1) incorporation of silver d electrons in the delocalized conjugated π system network of the acetylides and (2) the extent of the π delocalization. On the basis of these results, a set of design strategies and stereochemical and electronic principles have been developed in order to improve the third-order nonlinear optical responses. Specifically, the $\chi^{(3)}$ and γ values of an organometallic polymer can be significantly enhanced by utilizing a highly polarizable metal atom (e.g., a d^{10} transition metal) with an extended π conjugation organic system, coupled with a low MLCT excitation energy, an asymmetric metal coordination, and a large degree of oligomerization. Work is in progress to employ these strategies to design a whole new class of nonlinear optical materials based on the novel multiple (double, triple, and quadruple) salts of silver described in the previous section. The ease of incorporating desirable substituents on the acetylide and other anions or ligands coordinated to the silver ions of these multiple silver salts makes this interesting class of nonlinear optical materials highly tailorable.

Acknowledgment. We are grateful to the National Science Foundation, USA (Materials Initiative Grant to B.K.T.) for financial support of this research.

IC010408C